

# Invalidation of dieckol and 1,2,3,4,6-pentagalloylglucose (PGG) as SARS-CoV-2 main protease inhibitors and the discovery of PGG as a papain-like protease inhibitor

Haozhou Tan

Rutgers University New Brunswick

Chunlong Ma

University of Arizona College of Pharmacy: The University of Arizona College of Medicine Phoenix

Jun Wang (✉ [junwang@pharmacy.rutgers.edu](mailto:junwang@pharmacy.rutgers.edu))

Rutgers The State University of New Jersey <https://orcid.org/0000-0002-4845-4621>

---

## Research Article

**Keywords:** SARS-CoV-2, main protease, papain-like protease, antiviral, coronavirus

**Posted Date:** March 30th, 2022

**DOI:** <https://doi.org/10.21203/rs.3.rs-1490282/v1>

**License:**   This work is licensed under a Creative Commons Attribution 4.0 International License.

[Read Full License](#)

---

# Abstract

The COVID-19 pandemic spurred a broad interest in antiviral drug discovery. The SARS-CoV-2 main protease ( $M^{pro}$ ) and papain-like protease ( $PL^{pro}$ ) are attractive antiviral drug targets given their vital roles in viral replication and modulation of host immune response. Structurally disparate compounds were reported as  $M^{pro}$  and  $PL^{pro}$  inhibitors from either drug repurposing or rational design. Two polyphenols dieckol and 1,2,3,4,6-pentagalloylglucose (PGG) were recently reported as SARS-CoV-2 main protease ( $M^{pro}$ ) inhibitors. With our continuous interest in studying the mechanism of inhibition and resistance of  $M^{pro}$  inhibitors, we report herein our independent validation/invalidation of these two natural products. Our FRET-based enzymatic assay showed that neither dieckol nor PGG inhibited SARS-CoV-2  $M^{pro}$  ( $IC_{50} > 20 \mu M$ ), which is in contrary to previous reports. Serendipitously, PGG was found to inhibit the SARS-CoV-2 papain-like protease ( $PL^{pro}$ ) with an  $IC_{50}$  of  $3.90 \mu M$ . The binding of PGG to  $PL^{pro}$  was further confirmed in the thermal shift assay. However, PGG was cytotoxic in 293T-ACE2 cells ( $CC_{50} = 7.7 \mu M$ ), so its intracellular  $PL^{pro}$  inhibitory activity could not be quantified by the cell-based Flip-GFP  $PL^{pro}$  assay. In addition, we also invalidated ebselen, disulfiram, carmofur, PX12, and tideglusib as SARS-CoV-2  $PL^{pro}$  inhibitors using the Flip-GFP assay. Overall, our results call for stringent hit validation, and the serendipitous discovery of PGG as a putative  $PL^{pro}$  inhibitor might worth further pursuing.

## Introduction

COVID-19 is caused by the SARS-CoV-2, an enveloped, single-stranded, and positive-sense RNA virus [1]. Seven coronaviruses are known to infect humans including four common human coronaviruses OC43, 229E, NL63, and HKU1, and three highly pathogenic coronaviruses SARS-CoV, SARS-CoV-2 and MERS-CoV [2]. The COVID-19 pandemic is a timely call for the urgent need of orally bioavailable antivirals. Drug repurposing plays a pivotal role in advancing drug candidates to clinic [3]. For example, the first FDA-approved COVID drug, remdesivir, was originally developed for Ebola virus [4], and was later found to have broad-spectrum antiviral activity against several viruses including SARS-CoV, MERS-CoV, and SARS-CoV-2 [5, 6]. Similarly, molnupiravir was a clinical candidate for the influenza virus before repurposed for SARS-CoV-2 [7, 8]. The SARS-CoV-2 main protease ( $M^{pro}$ ) and papain-like protease ( $PL^{pro}$ ) are also high-profile drug targets for drug repurposing. Numerous virtual screenings and high-throughput screenings have been conducted, revealing structurally disparate inhibitors that are at different stages of preclinical and clinical development [9]. For example, boceprevir [10, 11], calpain inhibitors [10], GC-376 [10, 12], and masitinib [13] were among the first hits reported as  $M^{pro}$  inhibitors. GRL0617 [14, 15], YM155 [16], 6-thioguanine [17], SJB2-043 [18], and others were identified as  $PL^{pro}$  inhibitors. Natural products are also a rich source of modern medicine [19], and multiple natural products have been reported as  $M^{pro}$  and  $PL^{pro}$  inhibitors [20]. For example, two polyphenols dieckol and 1,2,3,4,6-pentagalloylglucose (PGG) were recently reported as SARS-CoV-2 main protease ( $M^{pro}$ ) inhibitors [21, 22]. With our continuous interest in validation/invalidation of literature reported SARS-CoV-2  $M^{pro}$  and  $PL^{pro}$  inhibitors [23–26], we report herein our independent validation of these two compounds using the established FRET enzymatic assay

and cell-based Flip-GFP assay. In addition, we further confirmed that the previously reported promiscuous cysteine modifiers ebselen, disulfiram, carmofur, PX12, and tideglusib [27] are not PL<sup>pro</sup> inhibitors, despite the claim from several publications that they act as PL<sup>pro</sup> inhibitors [28, 29]. Interestingly, we serendipitously discovered PGG as a PL<sup>pro</sup> inhibitor and showed that PGG binds to PL<sup>pro</sup> and inhibited the enzymatic activity of PL<sup>pro</sup> in the FRET assay. Taken together, our results call for stringent hit validation, and the serendipitous discovery of PGG as a putative PL<sup>pro</sup> inhibitor might worth further investigation.

## Results And Discussion

### Invalidation of dieckol and PGG as SARS-CoV-2 M<sup>pro</sup> inhibitors.

Dieckol was reported as a SARS-CoV-2 M<sup>pro</sup> inhibitor through a fluorescence polarization-based high-throughput screening [21]. In the assay design, the biotin-labeled M<sup>pro</sup> substrate was conjugated with a fluorescein isocyanate (FITC) fluorophore, resulting in a bifunctional probe FITC-AVLQ↓SGFRKK-Biotin (FITC-S-Biotin). Binding of this probe to avidin led to increased fluorescence polarization. Upon M<sup>pro</sup> digestion, the fluorophore-peptide conjugate FITC-AVLQ was released, which correlates with reduced millipolarization unit (mP) signal. Screening of a natural product library of 5,000 compounds identified dieckol as a potent M<sup>pro</sup> inhibitor with IC<sub>50</sub> values of 4.5 μM (no DTT) and 2.9 μM (1 mM DTT). The mechanism of action was characterized using the FRET assay and surface plasmon resonance binding assay, both of which showed consistent results as the FP assay. Enzymatic kinetic studies demonstrated that dieckol is a competitive M<sup>pro</sup> inhibitor. It is noted that dieckol was also previously reported as a SARS-CoV M<sup>pro</sup> inhibitor [30].

PGG was reported as an inhibitor for both SARS-CoV and SARS-CoV-2 M<sup>pro</sup> with IC<sub>50</sub> values of 6.89 and 3.66 μM, respectively [22]. In another study, PGG was found to bind to the SARS-CoV-2 spike protein receptor binding domain (RBD) with a K<sub>D</sub> of 6.69 μM in the bio-layer interferometry assay, while the binding of PGG to the ACE2 receptor was weaker with a K<sub>D</sub> of 22.2 μM [31]. PGG was further shown to block the RBD-ACE2 interactions in the ELISA assay with an IC<sub>50</sub> of 46.9 μM. In the SARS-CoV-2 pseudovirus assay, PGG dose-dependently inhibited the viral entry and replication.

To validate whether dieckol and PGG are M<sup>pro</sup> inhibitors, we repeated the FRET enzymatic assay using our standard FRET assay condition (20 mM HEPES, pH 6.5, 120 mM NaCl, 0.4 mM EDTA, 4 mM DTT, and 20% glycerol). Both dieckol and PGG were inactive (IC<sub>50</sub> > 20 μM) (Table 1). To examine whether dieckol and PGG inhibited the intracellular protease activity of M<sup>pro</sup>, we characterized both compounds in the cell-based Flip-GFP M<sup>pro</sup> assay. Our previous results showed that there is generally a positive correlation between the Flip-GFP and antiviral assay results, while the correlation between the FRET enzymatic assay results and antiviral assay results is compound dependent [15]. In the Flip-GFP assay, the GFP is reconstituted upon cleavage of the engineered linker by M<sup>pro</sup>, and the normalized GFP/mCherry signal ratio is proportional to the M<sup>pro</sup> activity (mCherry serves as an internal control for the protein expression

level or compound toxicity) [32, 33]. GC-376 was included as a positive control and it showed an EC<sub>50</sub> of 3.5 μM (Fig. 1A). The results showed that both compounds lacked the cellular M<sup>pro</sup> inhibitory activity at non-toxic drug concentrations (Fig. 1A). Dieckol was not active (IC<sub>50</sub> > 60 μM), while PGG was cytotoxic (CC<sub>50</sub> = 9.8 μM) (Fig. 1A), therefore the result was not conclusive. Taken together, dieckol and PGG were both invalidated as M<sup>pro</sup> inhibitors.

In parallel, we tested dieckol and PGG against SARS-CoV-2 PL<sup>pro</sup> in the FRET assay. While dieckol was not active (IC<sub>50</sub> > 20 μM), PGG was serendipitously found to inhibit SARS-CoV-2 PL<sup>pro</sup> with an IC<sub>50</sub> of 3.9 μM (Fig. 1B and Table 1). To profile the broad-spectrum activity, PGG was tested against SARS-CoV and MERS-CoV PL<sup>pro</sup>. PGG showed weak activity against SARS-CoV PL<sup>pro</sup> with an IC<sub>50</sub> of 12.3 μM, while it was inactive against the MERS-CoV (IC<sub>50</sub> > 60 μM) (Fig. 1B). These results suggest that the inhibition of SARS-CoV-2 PL<sup>pro</sup> by PGG might be specific. We further characterized the binding of PGG to SARS-CoV-2 PL<sup>pro</sup> in the thermal shift assay and found that PGG increased the thermal stability of PL<sup>pro</sup> in a dose dependent manner (Fig. 1C). To determine whether PGG inhibits the intracellular protease activity of SARS-CoV-2 PL<sup>pro</sup>, we performed the Flip-GFP PL<sup>pro</sup> assay. Unfortunately, PGG was cytotoxic to the 293T cells used in the Flip-GFP PL<sup>pro</sup> assay (CC<sub>50</sub> = 7.7 μM), resulting in inconclusive results (Fig. 1D).

Table 1

Validation and invalidation of SARS-CoV-2 M<sup>pro</sup> and PL<sup>pro</sup> inhibitors.

Compound	Reported SARS-CoV-2 M <sup>pro</sup> inhibition IC <sub>50</sub> (μM)	Reported SARS-CoV-2 PL <sup>pro</sup> inhibition IC <sub>50</sub> (μM)	Validation results IC <sub>50</sub> (μM)
<b>Dieckol</b>	IC <sub>50</sub> = 4.5 ± 0.4 (1 mM DTT) IC <sub>50</sub> = 2.9 ± 0.2 (no DTT) Competitive inhibitor K <sub>i</sub> = 3.3 μM [21] SPR K <sub>D</sub> = 0.22 μM	N.A.	<b>FRET assay:</b> M <sup>pro</sup> IC <sub>50</sub> > 20 (4 mM DTT) PL <sup>pro</sup> IC <sub>50</sub> > 20 (4 mM DTT) <b>Flip-GFP M<sup>pro</sup> assay:</b> IC <sub>50</sub> > 60 μM
<b>PGG</b>	SARS-CoV-2 IC <sub>50</sub> = 3.66 ± 0.02 SARS-CoV IC <sub>50</sub> = 6.89 ± 0.15 [22]	N. A.	<b>FRET assay:</b> M <sup>pro</sup> IC <sub>50</sub> > 20 (4 mM DTT) PL <sup>pro</sup> IC <sub>50</sub> = 3.90 ± 1.10 (4 mM DTT) <b>Thermal shift assay:</b> ΔT <sub>m</sub> = 3.91 °C <b>Flip-GFP M<sup>pro</sup> assay:</b> IC <sub>50</sub> > 3 μM <b>Flip-GFP PL<sup>pro</sup> assay:</b> IC <sub>50</sub> > 3 μM
<b>Ebselen</b>	IC <sub>50</sub> = 3.7 ± 2.4 (4 mM DTT) IC <sub>50</sub> > 60 (4 mM DTT) [25]	IC <sub>50</sub> = 10.3 ± 8.9 (4 mM DTT) IC <sub>50</sub> > 60 (4 mM DTT) [25]	<b>Flip-GFP PL<sup>pro</sup> assay:</b> IC <sub>50</sub> > 30 μM
<b>Disulfiram</b>	IC <sub>50</sub> = 2.1 ± 0.3 (4 mM DTT) IC <sub>50</sub> > 60 (4 mM DTT) [25]	IC <sub>50</sub> = 6.9 ± 4.2 (4 mM DTT) IC <sub>50</sub> > 60 (4 mM DTT) [25]	<b>Flip-GFP PL<sup>pro</sup> assay:</b> IC <sub>50</sub> > 10 μM

N.A. = not available.

Compound	Reported SARS-CoV-2 M <sup>pro</sup> inhibition IC <sub>50</sub> (μM)	Reported SARS-CoV-2 PL <sup>pro</sup> inhibition IC <sub>50</sub> (μM)	Validation results IC <sub>50</sub> (μM)
<b>Carmofur</b>	IC <sub>50</sub> = 0.2 ± 0.1 (4 mM DTT) IC <sub>50</sub> = 28.2 ± 9.5 (4 mM DTT) [25]	IC <sub>50</sub> = 0.7 ± 0.1 (4 mM DTT) IC <sub>50</sub> > 60 (4 mM DTT) [25]	<b>Flip-GFP PL<sup>pro</sup> assay:</b> IC <sub>50</sub> > 50 μM
<b>PX-12</b>	IC <sub>50</sub> = 0.9 ± 0.2 (4 mM DTT) IC <sub>50</sub> > 60 (4 mM DTT) [25]	IC <sub>50</sub> = 18.7 ± 2.6 (4 mM DTT) IC <sub>50</sub> > 60 (4 mM DTT) [25]	<b>Flip-GFP PL<sup>pro</sup> assay:</b> IC <sub>50</sub> > 50 μM
<b>Tideglusib</b>	IC <sub>50</sub> = 2.1 ± 0.3 (4 mM DTT) IC <sub>50</sub> > 60 (4 mM DTT) [25]	IC <sub>50</sub> = 7.1 ± 1.4 (4 mM DTT) IC <sub>50</sub> = 30.4 ± 17.1 (4 mM DTT) [25]	<b>Flip-GFP PL<sup>pro</sup> assay:</b> IC <sub>50</sub> > 60 μM
N.A. = not available.			

To gain insights of the binding mode, we performed molecular docking of PGG with SARS-CoV-2 PL<sup>pro</sup> (PDB: 7JRN) [15] using the Schrödinger Glide extra-precision. The binding sites in PL<sup>pro</sup> were determined by the sitemap, which revealed the BL2 loop region as the highest-ranking binding site, therefore it was selected for PGG docking. The BL2 loop region is also the drug binding site of the known PL<sup>pro</sup> inhibitors GRL0617 [15]. Docking results showed that PGG fits snugly in the binding site with a Glide score of -10.024 (Fig. 2A). PGG formed multiple hydrogen bonds with PL<sup>pro</sup> residues including the side chains of Tyr273, Asp302, Arg166, Lys157 and the main chain of Leu162 (Fig. 2B).

#### **Invalidation of disulfiram, ebselen, carmofur, PX-12, and tideglusib as SARS-CoV-2 PL<sup>pro</sup> inhibitors.**

Disulfiram was previously reported as a PL<sup>pro</sup> inhibitor of both SARS-CoV and MERS-CoV [28]. Enzymatic kinetic studies showed that disulfiram acts as an allosteric inhibitor of MERS-CoV PL<sup>pro</sup> and a competitive inhibitor of the SARS-CoV PL<sup>pro</sup>. In contrary, our previous study revealed that the inhibition of SARS-CoV-2 PL<sup>pro</sup> by ebselen in the FRET-based enzymatic assay is reducing reagent dependent [25]. Ebselen inhibited SARS-CoV-2 PL<sup>pro</sup> with an IC<sub>50</sub> of 6.9 μM in the absence of DTT but was not active in the presence of DTT (IC<sub>50</sub> > 60 μM) (Table 1). Likewise, ebselen, carmofur, PX-12, and tideglusib all showed various degrees of inhibition against the SARS-CoV-2 PL<sup>pro</sup> in the absence of DTT, while the inhibition was abolished in the presence of DTT (Table 1) [25]. In contrary, Weglarz-Tomczak et al reported that ebselen inhibited SARS-CoV and SARS-CoV-2 PL<sup>pro</sup>s with IC<sub>50</sub> values of 8.45 and 2.26 μM, respectively, in the presence of 2 mM DTT [29]. Disulfiram and ebselen were also proposed to inhibit SARS-CoV-2 PL<sup>pro</sup> through ejecting zinc from the zinc-binding domain [34]. Given the debate whether

reducing reagent should be added to the cysteine protease assay buffer, coupled with the controversy FRET assay results of ebselen in the presence of DTT, we were interested in further characterizing the inhibition of SARS-CoV-2 PL<sup>pro</sup> by these compounds in a native cellular environment. For this, we employed our recently established cellular Flip-GFP PL<sup>pro</sup> assay [15] to test the intracellular activity of these compounds. It was found that none of the compounds tested reduced the GFP/mCherry ratio at non-cytotoxic concentrations (Fig. 3), suggesting they lack the intracellular target engagement and PL<sup>pro</sup> inhibition. Collectively, our data suggest that disulfiram, ebselen, carmofur, PX-12, and tideglusib should not be classified as PL<sup>pro</sup> inhibitors.

## Conclusion

In conclusion, our data suggested that dieckol and PGG are not M<sup>pro</sup> inhibitors as shown from the FRET and Flip-GFP M<sup>pro</sup> assays. Furthermore, the previously reported promiscuous cysteine modifiers ebselen, disulfiram, carmofur, PX-12, and tideglusib were also invalidated as PL<sup>pro</sup> inhibitors by the Flip-GFP PL<sup>pro</sup> assay. Taken together with our previous efforts in invalidating these compounds as M<sup>pro</sup> inhibitors, it can be concluded that M<sup>pro</sup> and PL<sup>pro</sup> enzymatic assay results obtained in the absence of reducing reagents have no correlation with their cellular activity. Among the list of compounds examined, ebselen was previously shown to inhibit SARS-CoV-2 viral replication in cell culture [27, 35]. Coupled with the results presented here, it appears that the antiviral mechanism of action of ebselen is independent of either M<sup>pro</sup> or PL<sup>pro</sup> inhibition.

Since the FRET assay conditions used in different labs vary, it might be challenging to directly compare the results. Nonetheless, the cell-based Flip-GFP assay is a valuable tool in evaluating the intracellular protease activity and is a close mimetic of virus-infected cells.

In summary, the results presented herein call for stringent hit validation before investing resources for lead optimization and translational antiviral development. The discovery of PGG as a PL<sup>pro</sup> inhibitor provides another starting point for further optimization.

## Materials And Methods

All compounds were purchased from commercial source without further purification. PGG was ordered from Toronto Research Chemical with the Cat # P270450.

**SARS-CoV-2 M<sup>pro</sup> and PL<sup>pro</sup> expression and purification.** SARS-CoV-2 main protease (M<sup>pro</sup>) gene from strain BetaCoV/Wuhan/WIV04/2019 (GenBank: MN996528.1) was purchased from GenScript (Piscataway, NJ) with *E. coli* codon optimization and inserted into pET29a(+) plasmid. The M<sup>pro</sup> genes were then subcloned into the pE-SUMO plasmid as previously described [10, 36]. The expression and purification procedures were previously described [10]. SARS-CoV-2 papain-like protease (PL<sup>pro</sup>) gene (ORF 1ab 1564–1876) from strain BetaCoV/Wuhan/WIV04/2019 with *Escherichia coli* codon

optimization was ordered from GenScript in the pET28b(+) vector. The detailed expression and purification procedures were previously described [15].

**FRET-Based Enzymatic Assay.** For the  $IC_{50}$  measurement with the FRET-based assay, the reaction was carried out in 96-well format with 100  $\mu$ L of 200 nM PL<sup>pro</sup> protein in a PL<sup>pro</sup> reaction buffer (50 mM HEPES (pH 7.5), 5 mM DTT, and 0.01% Triton X-100); 1  $\mu$ L of testing compounds at various concentrations was added to each well and was incubated at 30°C for 30 min. The reaction was initiated by adding 1  $\mu$ L of 1 mM FRET substrate and was monitored in a Cytation 5 image reader with filters for excitation at 360/40 nm and emission at 460/40 nm at 30°C for 1 h. The initial velocity of the enzymatic reaction was calculated from the initial 10 min enzymatic reaction. The  $IC_{50}$  was calculated by plotting the initial velocity against various concentrations of testing compounds using a four-parameter variable slope dose – response curve in Prism 8 software.  $IC_{50}$  values for the testing compounds against SARS-CoV-2 M<sup>pro</sup> was determined as previously described [10].

**Flip-GFP M<sup>pro</sup> and PL<sup>pro</sup> assay.** Plasmid pcDNA3-TEV-FlipGFP-T2A-mCherry was ordered from Addgene (catalog No.124429). pcDNA3 FlipGFP-M<sup>pro</sup> plasmid and pcDNA3 FlipGFP-PL<sup>pro</sup> plasmid were constructed by introducing SARS-CoV-2 M<sup>pro</sup> cleavage site AVLQSGFR and SARS-CoV-2 PL<sup>pro</sup> cleavage site LRGGAPTK, respectively, via overlapping PCRs. pLVX SARS-CoV-2 M<sup>pro</sup> and pcDNA3.1 SARS-CoV-2 PL<sup>pro</sup> plasmids was ordered from Genescript (Piscataway NJ) with codon optimization.

The Flip-GFP M<sup>pro</sup> and PL<sup>pro</sup> assays were performed as previous reported [15, 23, 24, 37]. Briefly, the assay started with seeding 293T-ACE2 in 96-well, black, clear bottomed plate (Greiner, catalog No.655090) and incubating overnight to allow cells to reach 70–80% confluency. 50 ng of pLVX SARS-CoV-2 M<sup>pro</sup> (or pcDNA3.1 SARS-CoV-2 PL<sup>pro</sup>) and 50 ng of pcDNA3 FlipGFP- M<sup>pro</sup> (or pcDNA3 FlipGFP-PL<sup>pro</sup>) reporter plasmid was mixed with transfection reagent TransIT-293 (Mirus, catalog No. MIR 2700). The mixture was then transfected to each well according to manufacturer's instructions. After 2.5-3 hours of incubation in 37°C, 1  $\mu$ L of testing compound was added into each well directly and mixed by gentle plate shaking. 48 hours post transfection, fluorescence was quantified using SpectraMax iD3 plate reader (Molecular Devices) and images were taken using BZ-X800E fluorescence microscope (Keyence) in GFP and mCherry channels at 4X objective lens.

**Differential Scanning Fluorimetry (DSF).** The thermal shift binding assay (TSA) was carried out using a Thermo Fisher QuantStudio 5 Real-Time PCR system as described previously [10].

**Molecular docking.** Docking of PGG in SARS-CoV-2 PL<sup>pro</sup> was performed using the Schrödinger Glide extra precision program. The X-ray crystal structure of SARS-CoV-2 PL<sup>pro</sup> in complex with GRL0617 (PDB: 7JRN) was chosen for the docking. The gride box was centered on GRL0617. The docking poses were visualized using Pymol.

## Declarations



## Acknowledgements

This research was supported by the National Institutes of Health (NIH) (grants AI147325, AI157046, and AI158775) to J.W.

## Compliance with ethical standards

## Conflict of interest

The authors declare no competing interests.

## References

1. Hu B, Guo H, Zhou P, Shi ZL (2021) Characteristics of SARS-CoV-2 and COVID-19. *Nat Rev Microbiol* 19(3):141–154. <https://doi:10.1038/s41579-020-00459-7>
2. V'kovski P, Kratzel A, Steiner S, Stalder H, Thiel V (2021) Coronavirus biology and replication: implications for SARS-CoV-2. *Nat Rev Microbiol* 19(3):155–170. <https://doi:10.1038/s41579-020-00468-6>
3. Gordon DE, Jang GM, Bouhaddou M, Xu J, Obernier K, White KM et al (2020) A SARS-CoV-2 protein interaction map reveals targets for drug repurposing. *Nature* 583(7816):459–468. <https://doi:10.1038/s41586-020-2286-9>
4. Warren TK, Jordan R, Lo MK, Ray AS, Mackman RL, Soloveva V et al (2016) Therapeutic efficacy of the small molecule GS-5734 against Ebola virus in rhesus monkeys. *Nature* 531(7594):381–385. <https://doi:10.1038/nature17180>
5. Sheahan TP, Sims AC, Graham RL, Menachery VD, Gralinski LE, Case JB et al (2017) Broad-spectrum antiviral GS-5734 inhibits both epidemic and zoonotic coronaviruses. *Sci Transl Med* 9(396). <https://doi:10.1126/scitranslmed.aal3653>
6. Eastman RT, Roth JS, Brimacombe KR, Simeonov A, Shen M, Patnaik S et al (2020) Remdesivir: A Review of Its Discovery and Development Leading to Emergency Use Authorization for Treatment of COVID-19. *ACS Cent Sci* 6(5):672–683. <https://doi:10.1021/acscentsci.0c00489>
7. Cox RM, Wolf JD, Plemper RK (2021) Therapeutically administered ribonucleoside analogue MK-4482/EIDD-2801 blocks SARS-CoV-2 transmission in ferrets. *Nat Microbiol* 6(1):11–18. <https://doi:10.1038/s41564-020-00835-2>
8. Toots M, Yoon J-J, Cox RM, Hart M, Sticher ZM, Makhsous N et al (2019) Characterization of orally efficacious influenza drug with high resistance barrier in ferrets and human airway epithelia. *Sci Transl Med* 11(515):eaax5866. <https://doi:10.1126/scitranslmed.aax5866>
9. Ghosh AK, Brindisi M, Shahabi D, Chapman ME, Mesecar AD (2020) Drug Development and Medicinal Chemistry Efforts toward SARS-Coronavirus and Covid-19 Therapeutics. *ChemMedChem* 15(11):907–932. <https://doi:10.1002/cmdc.202000223>

10. Ma C, Sacco MD, Hurst B, Townsend JA, Hu Y, Szeto T, Boceprevir et al (2020) GC-376, and calpain inhibitors II, XII inhibit SARS-CoV-2 viral replication by targeting the viral main protease. *Cell Res* 30(8):678–692. <https://doi.org/10.1038/s41422-020-0356-z>
11. Fu L, Ye F, Feng Y, Yu F, Wang Q, Wu Y et al (2020) Both Boceprevir and GC376 efficaciously inhibit SARS-CoV-2 by targeting its main protease. *Nat Commun* 11(1):4417. <https://doi.org/10.1038/s41467-020-18233-x>
12. Vuong W, Khan MB, Fischer C, Arutyunova E, Lamer T, Shields J et al (2020) Feline coronavirus drug inhibits the main protease of SARS-CoV-2 and blocks virus replication. *Nat Commun* 11(1):4282. <https://doi.org/10.1038/s41467-020-18096-2>
13. Drayman N, DeMarco JK, Jones KA, Azizi S-A, Froggatt HM, Tan K et al (2021) Masitinib is a broad coronavirus 3CL inhibitor that blocks replication of SARS-CoV-2. *Science* 373(6557):931–936. <https://doi.org/10.1126/science.abg5827>
14. Osipiuk J, Azizi SA, Dvorkin S, Endres M, Jedrzejczak R, Jones KA et al (2021) Structure of papain-like protease from SARS-CoV-2 and its complexes with non-covalent inhibitors. *Nat Commun* 12(1):743. <https://doi.org/10.1038/s41467-021-21060-3>
15. Ma C, Sacco MD, Xia Z, Lambrinidis G, Townsend JA, Hu Y et al (2021) Discovery of SARS-CoV-2 Papain-like Protease Inhibitors through a Combination of High-Throughput Screening and a FlipGFP-Based Reporter Assay. *ACS Cent Sci* 7(7):1245–1260. <https://doi.org/10.1021/acscentsci.1c00519>
16. Zhao Y, Du X, Duan Y, Pan X, Sun Y, You T et al (2021) High-throughput screening identifies established drugs as SARS-CoV-2 PLpro inhibitors. *Protein Cell* 12(11):877–888. <https://doi.org/10.1007/s13238-021-00836-9>
17. Swaim CD, Dwivedi V, Perng YC, Zhao X, Canadeo LA, Harastani HH et al (2021) 6-Thioguanine blocks SARS-CoV-2 replication by inhibition of PLpro. *iScience* 24(10):103213. <https://doi.org/10.1016/j.isci.2021.103213>
18. Cho CC, Li SG, Lalonde TJ, Yang KS, Yu G, Qiao Y et al (2022) Drug Repurposing for the SARS-CoV-2 Papain-Like Protease. *ChemMedChem* 17(1):e202100455. <https://doi.org/10.1002/cmdc.202100455>
19. Christy MP, Uekusa Y, Gerwick L, Gerwick WH (2021) Natural Products with Potential to Treat RNA Virus Pathogens Including SARS-CoV-2. *J Nat Prod* 84(1):161–182. <https://doi.org/10.1021/acs.jnatprod.0c00968>
20. Chakravarti R, Singh R, Ghosh A, Dey D, Sharma P, Velayutham R et al (2021) A review on potential of natural products in the management of COVID-19. *Rsc Adv* 11(27):16711–16735. <https://doi.org/10.1039/D1RA00644D>
21. Yan G, Li D, Lin Y, Fu Z, Qi H, Liu X et al (2021) Development of a simple and miniaturized sandwich-like fluorescence polarization assay for rapid screening of SARS-CoV-2 main protease inhibitors. *Cell & Bioscience* 11(1):199. <https://doi.org/10.1186/s13578-021-00720-3>
22. Chiou W-C, Chen J-C, Chen Y-T, Yang J-M, Hwang L-H, Lyu Y-S et al (2022) The inhibitory effects of PGG and EGCG against the SARS-CoV-2 3C-like protease. *Biochem Biophys Res Commun* 591:130–136. <https://doi.org/10.1016/j.bbrc.2020.12.106>

23. Ma C, Wang J (2022) Validation and Invalidation of SARS-CoV-2 Papain-like Protease Inhibitors. *ACS Pharmacol Transl Sci* 5(2):102–109. <https://doi:10.1021/acsptsci.1c00240>
24. Ma C, Tan H, Choza J, Wang Y, Wang J (2021) Validation and invalidation of SARS-CoV-2 main protease inhibitors using the Flip-GFP and Protease-Glo luciferase assays. *Acta Pharm Sinica B*. <https://doi:https://doi.org/10.1016/j.apsb.2021.10.026>
25. Ma C, Hu Y, Townsend JA, Lagarias PI, Marty MT, Kolocouris A et al (2020) Ebselen, Disulfiram, Carmofur, PX-12, Tideglusib, and Shikonin Are Nonspecific Promiscuous SARS-CoV-2 Main Protease Inhibitors. *ACS Pharmacol Transl Sci* 3(6):1265–1277. <https://doi:10.1021/acsptsci.0c00130>
26. Ma C, Wang J (2021) Dipyridamole, chloroquine, montelukast sodium, candesartan, oxytetracycline, and atazanavir are not SARS-CoV-2 main protease inhibitors. *Proc Natl Acad Sci U S A* 118(8):e2024420118. <https://doi:10.1073/pnas.2024420118>
27. Jin Z, Du X, Xu Y, Deng Y, Liu M, Zhao Y et al (2020) Structure of M(pro) from SARS-CoV-2 and discovery of its inhibitors. *Nature* 582(7811):289–293. <https://doi:10.1038/s41586-020-2223-y>
28. Lin MH, Moses DC, Hsieh CH, Cheng SC, Chen YH, Sun CY et al (2018) Disulfiram can inhibit MERS and SARS coronavirus papain-like proteases via different modes. *Antiviral Res* 150:155–163. <https://doi:10.1016/j.antiviral.2017.12.015>
29. Weglarz-Tomczak E, Tomczak JM, Talma M, Burda-Grabowska M, Giurg M, Brul S (2021) Identification of ebselen and its analogues as potent covalent inhibitors of papain-like protease from SARS-CoV-2. *Sci Rep* 11(1):3640. <https://doi:10.1038/s41598-021-83229-6>
30. Park J-Y, Kim JH, Kwon JM, Kwon H-J, Jeong HJ, Kim YM et al (2013) Dieckol, a SARS-CoV 3CLpro inhibitor, isolated from the edible brown algae *Ecklonia cava*. *Bioorg Med Chem* 21(13):3730–3737. <https://doi:https://doi.org/10.1016/j.bmc.2013.04.026>
31. Chen RH, Yang LJ, Hamdoun S, Chung SK, Lam CW-k, Zhang KX et al (2021) 1,2,3,4,6-Pentagalloyl Glucose, a RBD-ACE2 Binding Inhibitor to Prevent SARS-CoV-2 Infection. *Front Pharmacol* 12. <https://doi:10.3389/fphar.2021.634176>
32. Froggatt HM, Heaton BE, Heaton NS (2020) Development of a Fluorescence-Based, High-Throughput SARS-CoV-2 3CL(pro) Reporter Assay. *J Virol* 94(22):e01265–e01220. <https://doi:10.1128/JVI.01265-20>
33. Li X, Lidsky PV, Xiao Y, Wu CT, Garcia-Knight M, Yang J et al (2021) Ethacridine inhibits SARS-CoV-2 by inactivating viral particles. *PLoS Pathog* 17(9):e1009898. <https://doi:10.1371/journal.ppat.1009898>
34. Sargsyan K, Lin CC, Chen T, Grauffel C, Chen YP, Yang WZ et al (2020) Multi-targeting of functional cysteines in multiple conserved SARS-CoV-2 domains by clinically safe Zn-ejectors. *Chem Sci* 11(36):9904–9909. <https://doi:10.1039/d0sc02646h>
35. Amporndanai K, Meng X, Shang W, Jin Z, Rogers M, Zhao Y et al (2021) Inhibition mechanism of SARS-CoV-2 main protease by ebselen and its derivatives. *Nat Commun* 12(1):3061. <https://doi:10.1038/s41467-021-23313-7>

36. Sacco MD, Ma C, Lagarias P, Gao A, Townsend JA, Meng X et al (2020) Structure and inhibition of the SARS-CoV-2 main protease reveal strategy for developing dual inhibitors against M(pro) and cathepsin L. *Sci Adv* 6(50):eabe0751. <https://doi:10.1126/sciadv.abe0751>
37. Ma C, Xia Z, Sacco MD, Hu Y, Townsend JA, Meng X et al (2021) Discovery of Di- and Trihaloacetamides as Covalent SARS-CoV-2 Main Protease Inhibitors with High Target Specificity. *J Am Chem Soc* 143(49):20697–20709. <https://doi:10.1021/jacs.1c08060>

## Figures

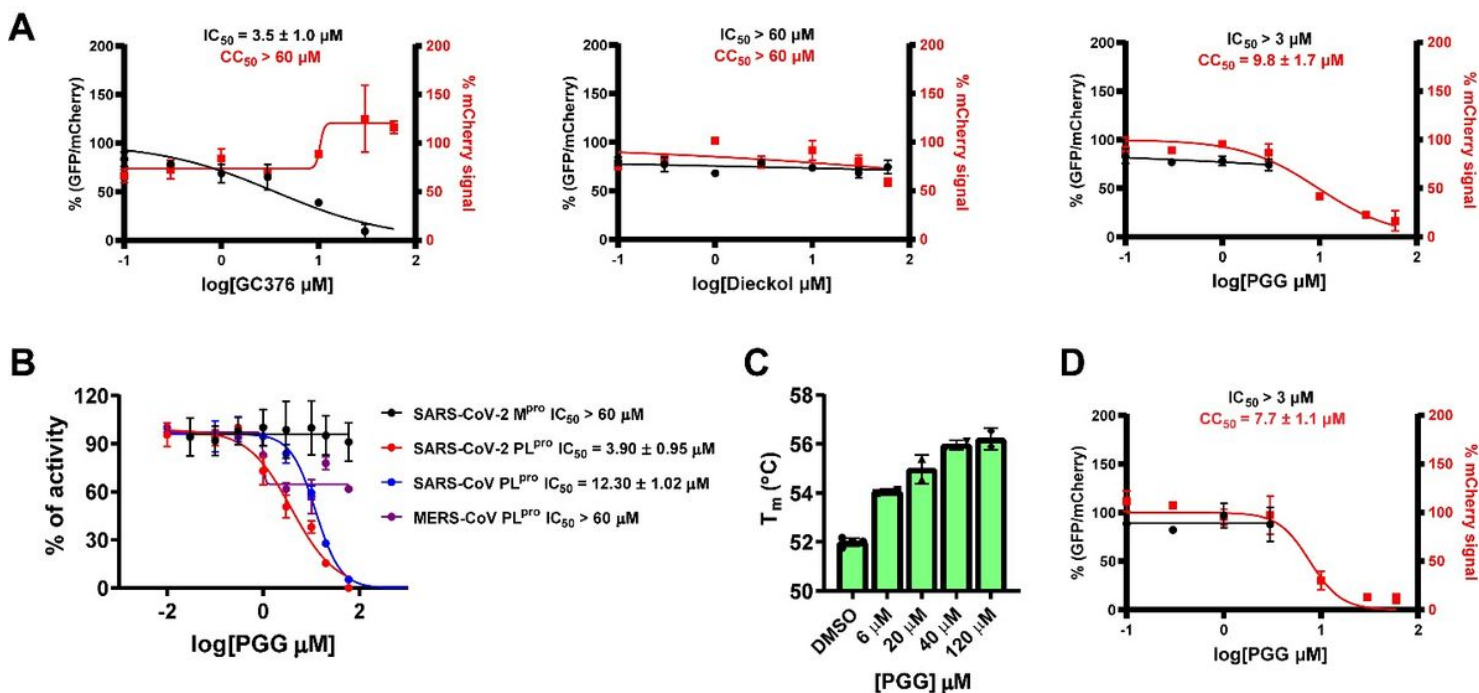
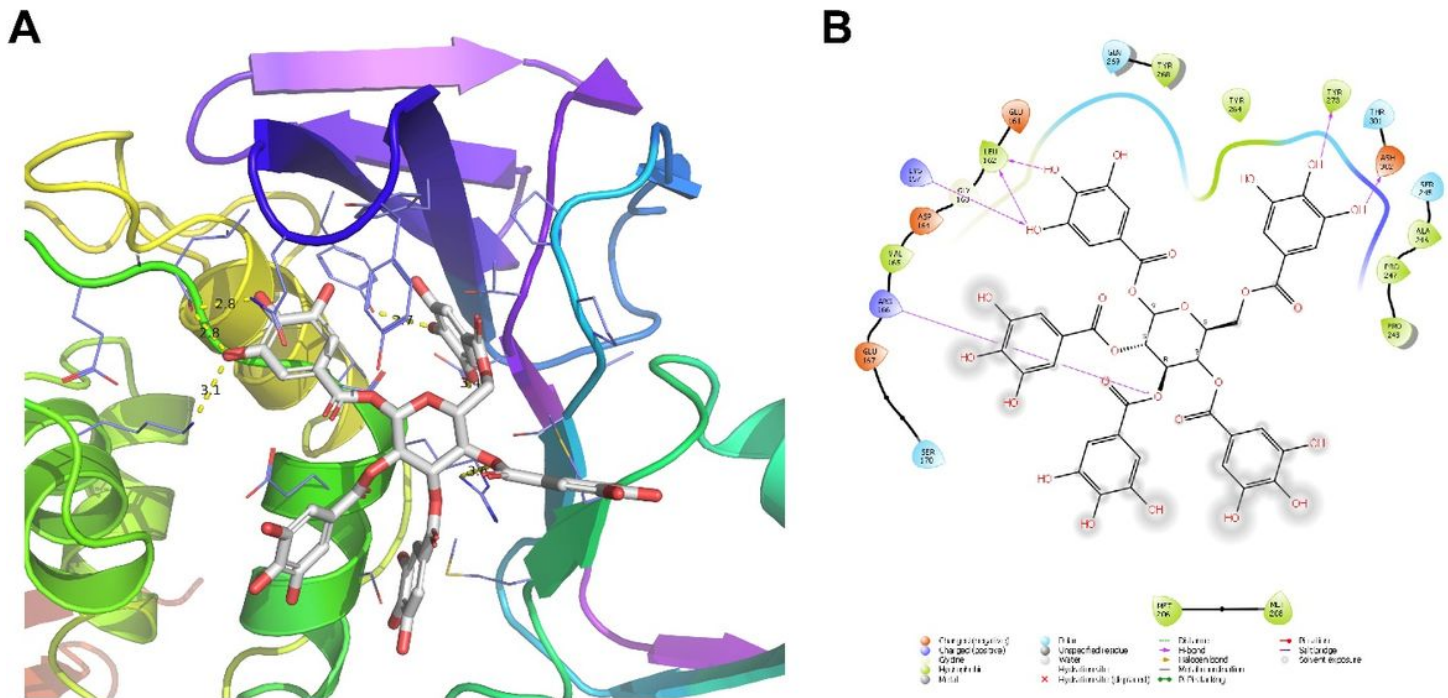


Figure 1

Validation and invalidation of dieckol and PGG as SARS-CoV-2 M<sup>pro</sup> and PL<sup>pro</sup> inhibitors. (A) Flip-GFP M<sup>pro</sup> assay results of dieckol and PGG. GC376 was included as a positive control. (B) FRET assay results of PGG against SARS-CoV-2 M<sup>pro</sup>, SARS-CoV-2 PL<sup>pro</sup>, SARS-CoV PL<sup>pro</sup>, and MERS-CoV PL<sup>pro</sup>. (C) Thermal shift assay characterization of the binding of PGG to SARS-CoV-2 PL<sup>pro</sup>. (D) Flip-GFP PL<sup>pro</sup> assay result of PGG. The results are mean  $\pm$  standard deviation of two repeats.



**Figure 2**

Docking model of PGG in SARS-CoV-2 PL<sup>pro</sup>. (A) Docking pose of PGG in the BL2 binding site of PL<sup>pro</sup>. (B) 2D ligand-protein interaction plot of PGG with SARS-CoV-2 PL<sup>pro</sup>. Docking was performed using the X-ray crystal structure of SARS-CoV-2 PL<sup>pro</sup> (PDB; 7JRN). The Glide score was -10.024 from the Schrödinger Glide extra-precision docking.

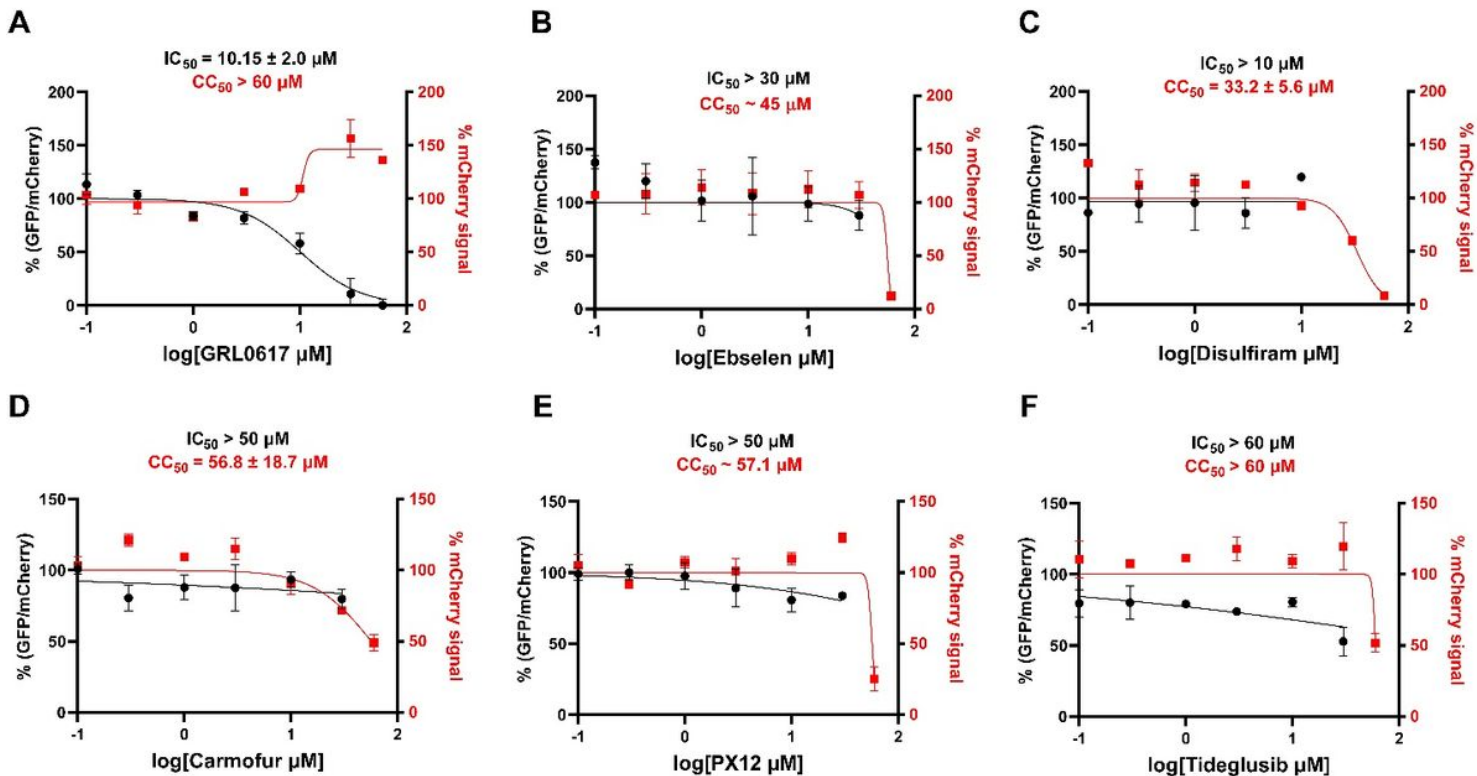


### Figure 3

SARS-CoV-2 Flip-GFP PL<sup>pro</sup> assay. GRL0617 (A) was included as a positive control. % (GFP/mCherry) ratio correlates with intracellular PL<sup>pro</sup> activity, and % mCherry signal correlates with compound toxicity or transfection efficiency. The results are mean  $\pm$  standard deviation of two repeats.

## Supplementary Files

This is a list of supplementary files associated with this preprint. Click to download.

- [Graphicabstract.jpg](#)